

AD-A142 551

AN INTEGRAL PREDICTION METHOD FOR THREE-DIMENSIONAL  
FLOW SEPARATION(U) DAVID W TAYLOR NAVAL SHIP RESEARCH  
AND DEVELOPMENT CENTER BET. T C TAI MAY 84 AERO-1292  
DTNSRDC-84/034

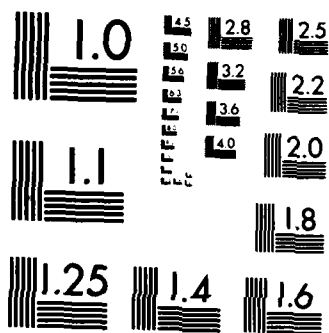
1/1

UNCLASSIFIED

F/G 20/4

NL





MICROCOPY RESOLUTION TEST CHART  
NATIONAL BUREAU OF STANDARDS-1963-A

12

DTNSRDC-84/034

**DAVID W. TAYLOR NAVAL SHIP  
RESEARCH AND DEVELOPMENT CENTER**

Bethesda, Maryland 20084



**AD-A142 551**

**AN INTEGRAL PREDICTION METHOD FOR  
THREE-DIMENSIONAL FLOW SEPARATION**

by

**T. C. Tai**

**APPROVED FOR PUBLIC RELEASE: DISTRIBUTION UNLIMITED**

Presented as Paper AIAA-84-0014 at the  
22nd Aerospace Sciences Meeting  
Reno, Nevada, on 9-12 January 1984

**AVIATION AND SURFACE EFFECTS DEPARTMENT  
RESEARCH AND DEVELOPMENT REPORT**

May 1984

DTNSRDC-84/034

**DTIC FILE COPY**

**AN INTEGRAL PREDICTION METHOD FOR THREE-DIMENSIONAL FLOW SEPARATION**

UNCLASSIFIED

SECURITY CLASSIFICATION OF THIS PAGE (When Data Entered)

REPORT DOCUMENTATION PAGE		READ INSTRUCTIONS BEFORE COMPLETING FORM
1. REPORT NUMBER DTNSRDC-84/034	2. GOVT ACCESSION NO.	3. RECIPIENT'S CATALOG NUMBER
4. TITLE (and Subtitle) AN INTEGRAL PREDICTION METHOD FOR THREE-DIMENSIONAL FLOW SEPARATION		5. TYPE OF REPORT & PERIOD COVERED Oct 1982-Dec 1983
		6. PERFORMING ORG. REPORT NUMBER Aero Report 1292
7. AUTHOR(s) T. C. Tai		8. CONTRACT OR GRANT NUMBER(s)
9. PERFORMING ORGANIZATION NAME AND ADDRESS David W. Taylor Naval Ship Research and Development Center Bethesda, Maryland 20084		10. PROGRAM ELEMENT, PROJECT, TASK AREA & WORK UNIT NUMBERS (See reverse side)
11. CONTROLLING OFFICE NAME AND ADDRESS David W. Taylor Naval Ship Research and Development Center Bethesda, Maryland 20084		12. REPORT DATE May 1984
		13. NUMBER OF PAGES 13
14. MONITORING AGENCY NAME & ADDRESS (if different from Controlling Office) Naval Air Systems Command Code AIR-310D Washington, D.C. 20361		15. SECURITY CLASS. (of this report) UNCLASSIFIED
		15a. DECLASSIFICATION DOWNGRADING SCHEDULE
16. DISTRIBUTION STATEMENT (of this Report)  APPROVED FOR PUBLIC RELEASE: DISTRIBUTION UNLIMITED		
17. DISTRIBUTION STATEMENT (of the abstract entered in Block 20, if different from Report)		
18. SUPPLEMENTARY NOTES  Presented as Paper AIAA-84-0014 at the 22nd Aerospace Sciences Meeting, Reno, Nevada, on 9-12 January 1984.		
19. KEY WORDS (Continue on reverse side if necessary and identify by block number)  Three-Dimensional Flow Separation Integral Boundary-Layer Method Streamline Method		
20. ABSTRACT (Continue on reverse side if necessary and identify by block number)  A three-dimensional integral boundary-layer approach is developed and coupled with the streamline method for theoretically determining the vortex-type flow separation. The governing equations are solved in a streamwise system using a power-law profile for the streamwise flow and the Mager profile for the crossflow. The reduced ordinary system is then  (Continued on reverse side)		

DD FORM 1 JAN 73 1473

EDITION OF 1 NOV 65 IS OBSOLETE

S N 0102-LF-014-6601

UNCLASSIFIED

SECURITY CLASSIFICATION OF THIS PAGE (When Data Entered)

UNCLASSIFIED

SECURITY CLASSIFICATION OF THIS PAGE (When Data Entered)

(Block 10)

Program Element 61152N  
Task Area ZR 0230201  
Work Unit 1606-110

(Block 20 continued)

coupled with the streamline equation and integrated using the fourth-order Runge-Kutta scheme. Cross flow derivatives are evaluated and accounted for during the integration. A prolate spheroid at incidence in an incompressible turbulent flow is considered as a test case. Good comparison between the theory and the experiment has been observed for the case of  $\alpha = 10$  degrees. For the case of high incidence, the method predicts a qualitative trend but deviated quantitatively due to the large crossflow involved.

S/N 0102- LF- 014- 6601

UNCLASSIFIED

SECURITY CLASSIFICATION OF THIS PAGE (When Data Entered)

## TABLE OF CONTENTS

	Page
LIST OF FIGURES . . . . .	iii
ABSTRACT . . . . .	1
NOMENCLATURE . . . . .	1
INTRODUCTION . . . . .	1
CALCULATION OF VISCOUS STREAMLINES . . . . .	1
INTEGRAL SOLUTION TO THREE-DIMENSIONAL TURBULENT BOUNDARY LAYERS . . . . .	2
NUMERICAL INTEGRATION . . . . .	3
RESULTS AND DISCUSSION . . . . .	4
CONCLUDING REMARKS . . . . .	6
REFERENCES . . . . .	6
APPENDIX . . . . .	7
INITIAL DISTRIBUTION . . . . .	8

## LIST OF FIGURES

1 - Streamlines in a Boundary Layer . . . . .	2
2 - Coordinate Systems . . . . .	2
3 - Streamwise Boundary Layer Shape Factor of Flow over a Prolate Spheroid at $\alpha = 10$ Deg and $V_{\infty} = 45$ m/s . . . . .	4
4 - Streamwise Momentum Thickness of Flow over a Prolate Spheroid at $\alpha = 10$ Deg and $V_{\infty} = 45$ m/s . . . . .	4
5 - Streamwise Skin Friction Coefficients of Flow over a Prolate Spheroid at $\alpha = 10$ deg and $V_{\infty} = 45$ m/s . . . . .	4
6 - Direction of Wall Shear Stress of Flow over a Prolate Spheroid at $\alpha = 10$ deg and $V_{\infty} = 45$ m/s . . . . .	4
7 - Comparison of Calculated and External Inviscid Streamlines . . . . .	5
8 - Crossflow Velocity Profiles and Resulting Shear Stress Derivatives along Streamline $\eta = 3$ of Flow over a Prolate Spheroid at $\alpha = 10$ deg and $V_{\infty} = 45$ m/s . . . . .	5
9 - Crossflow Skin Friction Coefficients of Flow over a Prolate Spheroid at $\alpha = 10$ deg and $V_{\infty} = 45$ m/s . . . . .	5
10 - Flow Separation Pattern on a Prolate Spheroid at $\alpha = 10$ deg and $V_{\infty} = 45$ m/s . . . . .	6
11 - Flow Separation Pattern on a Prolate Spheroid at $\alpha = 20$ deg and $V_{\infty} = 45$ m/s . . . . .	6

# AIAA'84

**AIAA-84-0014**

## **An Integral Prediction Method for Three-Dimensional Flow Separation**

T.C. Tai, David Taylor Naval Ship R&D  
Center, Bethesda, MD

Accession For	
NTIS GRA&I	<input checked="" type="checkbox"/>
DTIC TAB	<input type="checkbox"/>
Unannounced	<input type="checkbox"/>
Justification	
By	
Distribution/	
Availability Codes	
Avail and/or	
Dist	Special
<b>A-1</b>	



**AIAA 22nd Aerospace Sciences Meeting**  
**January 9-12, 1984/Reno, Nevada**

Tsz C. Fan\*

David Taylor Naval Ship Research and Development Center  
Bethesda, Maryland 20084Abstract

A three-dimensional integral boundary-layer approach is developed and coupled with the streamline method for theoretically determining the vortex-type flow separation. The governing equations are solved in a streamwise system using a power-law profile for the streamwise flow and the Mager profile for the crossflow. The reduced ordinary system is then coupled with the streamline equation and integrated using the fourth-order Runge-Kutta scheme. Crossflow derivatives are evaluated and accounted for during the integration. A prolate spheroid at incidence in an incompressible turbulent flow is considered as a test case. Good comparison between the theory and the experiment has been observed for the case of  $\alpha = 10$  degrees. For the case of high incidence, the method predicts a qualitative trend but deviates quantitatively due to the large crossflow involved.

Nomenclature

- $a, b$  = major and minor axes of an ellipsoid  
 $C_E$  = entrainment coefficient, defined in Eq. (9)  
 $C_f$  = skin friction coefficient  
 $f$  = local body radial distance from the centerline  
 $H$  = shape factor,  $\delta_1/\theta_{11}$   
 $h$  =  $(H - 1)/2$   
 $h_1, h_2$  = metric coefficients for coordinates  $\xi, \eta$   
 $K_1$  = curvature parameter,  $\frac{1}{h_1 h_2} \frac{\partial h_1}{\partial \eta}$   
 $K_2$  = curvature parameter,  $\frac{1}{h_1 h_2} \frac{\partial h_2}{\partial \xi}$   
 $M$  = Mach number  
 $P$  = static pressure  
 $Re$  = Reynolds number,  $\rho V_\infty a / \mu$   
 $s, n$  = distance along and normal to a streamline  
 $U$  = velocity at edge of boundary layer  
 $u, v$  = velocity components in streamwise coordinates  
 $V_\infty$  = freestream velocity  
 $x, \phi$  = body-oriented orthogonal coordinates  
 $\bar{x}, \bar{y}, \bar{z}$  = Cartesian coordinates  
 $\alpha$  = angle of attack  
 $\beta$  = wall shear angle between external inviscid streamline and corresponding limiting streamline  
 $\gamma$  = ratio of specific heats  
 $\delta$  = boundary layer thickness  
 $\delta_1$  = streamwise displacement thickness  
 $= \int_0^\delta \left(1 - \frac{u}{U}\right) d\zeta$   
 $\delta_2$  = crosswise displacement thickness  
 $= \int_0^\delta -\frac{v}{U} d\zeta$   
 $\theta_{11}$  = streamwise momentum thickness  
 $= \int_0^\delta \left(1 - \frac{u}{U}\right) \frac{u}{U} d\zeta$

- $\theta_{12}$  = crossflow momentum thickness  
 $= \int_0^\delta \left(1 - \frac{u}{U}\right) \frac{v}{U} d\zeta$   
 $\theta_{21}$  = crossflow momentum thickness  
 $= \int_0^\delta \frac{u}{U} \frac{v}{U} d\zeta$   
 $\theta_{22}$  = crossflow momentum thickness  
 $= \int_0^\delta \left(\frac{v}{U}\right)^2 d\zeta$   
 $\theta$  = streamline angle  
 $\lambda$  =  $\tan \beta$   
 $\mu$  = viscosity  
 $\xi, \eta, \zeta$  = streamwise coordinates  
 $\rho$  = density  
 $\tau$  = shearing stress

Subscripts

- $w$  = wall  
 $\infty$  = freestream  
 $\xi, \eta$  =  $\xi, \eta$  direction

Introduction

In three-dimensional flows, the envelope of limiting streamlines has been used as the separation line. Thus defined, the determination of the separation line has been found to be very difficult analytically even with the most sophisticated numerical techniques available. For most flows of practical interest, however, the separation is of the vortex type where vortices are created as a result of the convergence of viscous streamlines above the line of separation. The line of separation can be properly determined by the envelope of viscous streamlines in the boundary layer.<sup>1</sup>

The problem, therefore, is to determine the realistic streamline pattern based on realistic pressure or shear stress, either by experimental measurements or by means of viscous-inviscid interactions. An attempt at using pure inviscid pressure along with a simple friction model has had limited success.<sup>2</sup> A more general theoretical method is yet to be developed. The purpose of this paper is to describe a theoretical procedure for determining the vortex-type flow separation using a three-dimensional integral boundary-layer solution coupled with the streamline method.<sup>1</sup> As opposed to the usual boundary-layer approach, this method deals with the convergence of streamlines rather than with the vanishing of skin friction. A prolate spheroid at incidence in an incompressible turbulent flow is considered as a test case.

Calculation of Viscous Streamlines

To simulate the physical flow so that the flow separation can be detected, it is necessary to consider the streamlines inside the boundary layer; see Fig. 1. It is assumed that the envelope of converging viscous streamlines is above, but close to, that of the converging wall-limiting streamlines. Therefore, the line of separation can be determined by the envelope of converging streamline equations derived earlier:<sup>1, 2</sup>

The research was supported by the Naval Air Systems Command (AIR-310D, AIRTASK WR023-02) and by the Independent Research Program at the David Taylor Naval Ship R&D Center.

\*Research Aerospace Engineer, Aviation and Surface Effects Department. Associate Fellow AIAA.

$$\frac{D\phi}{Ds} = \frac{\sin \theta}{f} \quad (1)$$

$$\frac{Dx}{Ds} = \cos \theta \quad (2)$$

$$\frac{D\theta}{Ds} = \frac{1}{\gamma M^2 P} \left( \frac{\partial P}{\partial x} \sin \theta - \frac{1}{f} \frac{\partial P}{\partial \phi} \cos \theta + \frac{\partial \tau_\eta}{\partial \xi} \right) - \frac{df \sin \theta}{dx f} \quad (3)$$

where conventional symbols have been used with geometric variables illustrated in Fig. 2. For incompressible flows, the potential flow solution<sup>1</sup> can be used for the pressure gradients  $\partial P / \partial x$  and  $\partial P / \partial \phi$  in Eq. (3). The problem, therefore, is to provide proper values for the shear stress derivative  $\partial \tau_\eta / \partial \xi$ .

#### Integral Solution to Three-Dimensional Turbulent Boundary Layers

A simple analytic model for the shear stress derivative has shown some promise.<sup>2</sup> However, in more general cases, where the flow separation is predominantly of the vortex type, a more rigorous theoretical form is in order. While it is not straightforward to derive a universal theoretical friction model, it is possible, in most cases, to provide the required friction values numerically. In so doing, the use of the integral method seems to be appropriate because of its compactness and compatibility with the streamline approach. The (longitudinal) integration can be performed along a streamline.

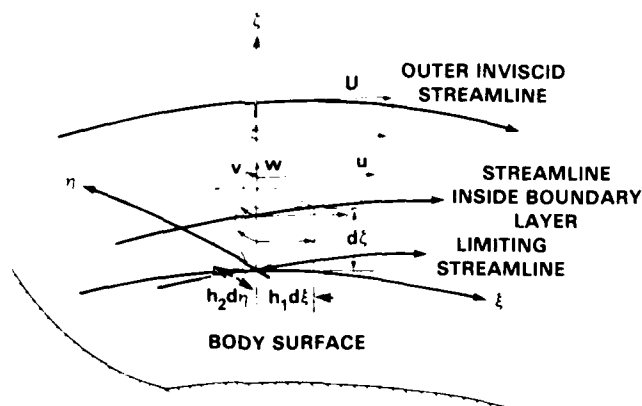


Fig. 1 - Streamlines in a boundary layer

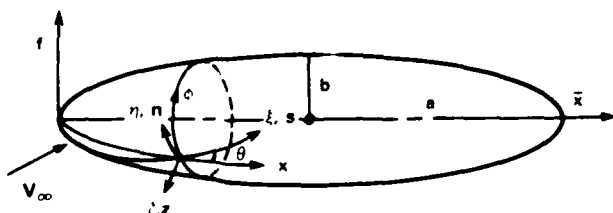


Fig. 2 - Coordinate systems

The integral equations for an incompressible, three-dimensional, turbulent boundary layer in streamwise coordinates are:

$\xi$  — momentum

$$\frac{1}{h_1} \frac{\partial \Theta_{11}}{\partial \xi} + \frac{1}{h_2} \frac{\partial \Theta_{12}}{\partial \eta} + \frac{2\Theta_{11}}{U h_1} \frac{\partial U}{\partial \xi} + \frac{1}{U h_2} \frac{\partial U}{\partial \eta} + (2\Theta_{21} + \delta_2) \left( \frac{1}{U h_2} \frac{\partial U}{\partial \eta} + K_1 \right) + (\Theta_{11} - \Theta_{22}) K_2 = \frac{\tau_\eta}{\rho U^2} \quad (4)$$

$\eta$  — momentum

$$\frac{1}{h_1} \frac{\partial \Theta_{21}}{\partial \xi} + \frac{1}{h_2} \frac{\partial \Theta_{22}}{\partial \eta} + 2\Theta_{21} \left( \frac{1}{U h_1} \frac{\partial U}{\partial \xi} + K_1 \right) + \frac{2\Theta_{22}}{U h_2} \frac{\partial U}{\partial \eta} + (\Theta_{11} - \Theta_{22} + \delta_1) K_1 = \frac{\tau_\eta}{\rho U^2} \quad (5)$$

Continuity

$$\frac{1}{h_1} \frac{\partial (\delta - \delta_1)}{\partial \xi} + \frac{1}{h_2} \frac{\partial \delta_2}{\partial \eta} + \left( K_2 + \frac{1}{U h_1} \frac{\partial U}{\partial \xi} \right) (\delta - \delta_1) - \left( K_1 + \frac{1}{U h_2} \frac{\partial U}{\partial \eta} \right) \delta_2 = C_t \quad (6)$$

To close the system, streamwise and crossflow velocity profiles, auxiliary relations for the skin friction, and flow entrainment are needed. The streamwise velocity profile is assumed to be the power-law form for two-dimensional flow; that is,

$$\frac{u}{U} = \left( \frac{z}{\delta} \right)^h$$

or

$$\bar{u} = z^h \quad (7)$$

where  $z = \xi / \delta$ ,  $h = (H - 1)/2$ , and  $H$  is the shape factor. The crossflow velocity profile takes the form suggested by Mager,<sup>4</sup>

$$\frac{v}{U} = \frac{u}{U} \left( 1 - \frac{z}{\delta} \right)^2 \tan \beta$$

or

$$\bar{v} = \bar{u} (1 - z)^2 \lambda \quad (8)$$

where  $\lambda = \tan \beta$ . The boundary-layer solution procedure in the present work is similar to that of Smith,<sup>5</sup> but differs in several aspects which will appear later.

The entrainment coefficient  $C_t$  is given as a function of the shape factor  $H$  by Green,<sup>6</sup> with the constant term being modified from 0.022 to 0.032:

$$C_t = 0.025H - 0.032 \quad (9)$$

The skin friction coefficient is related to the shape factor  $H$  and the Reynolds number based on the streamwise momentum thickness  $Re_{\Theta_{11}}$ ,<sup>6</sup>

$$\left( \frac{C_{ft}}{C_{f0}} + 0.5 \right) \left( \frac{H}{H_0} - 0.4 \right) = 0.9 \quad (10)$$

where  $C_{f0}$  and  $H_0$  are functions of  $Re_{\Theta_{11}}$ :

$$C_{f0} = \frac{0.01013}{2n Re_{\Theta_{11}} - 1.02} - 0.00075$$

$$H_0 = \frac{1}{1 - 6.55 \sqrt{0.5 C_{f0}}}$$

and the  $Re_{\Theta_{11}}$  and  $C_f$  are defined:

$$Re_{\Theta_{11}} = \frac{\rho U \Theta_{11}}{\mu}$$

$$C_f = \frac{\tau_w}{\frac{1}{2} \rho U^2}$$

The expressions for the curvature parameters  $K_1$  and  $K_2$  are derived in terms of quantities along a streamline. For  $K_1$ , the geometric relationship between two surface coordinate systems  $(x, \phi)$  and  $(\xi, \eta)$  is used:

$$\frac{\partial \phi}{\partial \xi} = \frac{h_1 \sin \theta}{f}; \quad \frac{\partial \phi}{\partial \eta} = \frac{h_2 \cos \theta}{f}$$

Taking cross differentiation and letting

$$\frac{\partial^2 \phi}{\partial \eta \partial \xi} = \frac{\partial^2 \phi}{\partial \xi \partial \eta}$$

result in

$$\begin{aligned} K_1 &= \frac{1}{h_1 h_2} \frac{\partial h_1}{\partial \eta} \\ &= \cot \theta \left( \frac{1}{h_1 h_2} \frac{\partial h_2}{\partial \xi} - \frac{1}{h_2} \frac{\partial \theta}{\partial \eta} - \frac{1}{f h_1} \frac{\partial f}{\partial \xi} \right) \\ &\quad - \frac{1}{h_1} \frac{\partial \theta}{\partial \xi} + \frac{1}{f h_2} \frac{\partial f}{\partial \eta} \\ &= \frac{1}{\gamma M^2 P} \left( -\frac{\partial P}{\partial x} \sin \theta + \frac{1}{f} \frac{\partial P}{\partial \phi} \cos \theta \right) \end{aligned} \quad (11)$$

where the sum of the three terms in parentheses is zero,<sup>7</sup> and the inviscid form of Eq. (3) has been used.

To find  $K_2$ , the continuity equation is written for the external flow in both the  $x, \phi$  coordinate system and the  $\xi, \eta$  system. By equating, there results

$$\begin{aligned} K_2 &= \frac{1}{h_1 h_2} \frac{\partial h_2}{\partial \xi} \\ &= \frac{1}{\gamma M^2 P} \left( \frac{\partial P}{\partial x} \cos \theta + \frac{1}{f} \frac{\partial P}{\partial \phi} \sin \theta \right) \end{aligned} \quad (12)$$

#### Numerical Integration

Equations (4) through (6), with the aid of Eqs. (7) through (12), allow solutions for three basic unknowns: the shape factor  $H$ , the streamwise displacement  $\Theta_{11}$ , and the tangent of the angle between the external inviscid streamline and the corresponding limiting streamline  $\lambda$ . These equations are recast into the form of streamwise derivatives:

$$\frac{DH}{Ds} = G_1 \quad (13)$$

$$\frac{D\Theta_{11}}{Ds} = G_2 \quad (14)$$

$$\frac{D\lambda}{Ds} = G_3 \quad (15)$$

where  $D/Ds = (1/h_1) \partial/\partial \xi$ , and  $G_1$ ,  $G_2$ , and  $G_3$  contain:

- (a) geometric properties and outer edge flow properties
- (b) variables  $H$ ,  $\Theta_{11}$ ,  $\lambda$ , etc. and
- (c) crossflow derivatives of  $H$ ,  $\Theta_{11}$ , and  $\lambda$

The detailed expressions for  $G_1$ ,  $G_2$ , and  $G_3$  are presented in the Appendix.

With the viscous solution in hand, the crossflow shear derivative required by Eq. (3) is obtained by differentiating Eq. (8) with the aid of the following relationships:

$$\begin{aligned} \tau_\eta &= \epsilon \frac{\partial v}{\partial \xi} \\ &= \frac{U \epsilon \lambda}{d} \left[ -2(1-z)\bar{u} + (1-z)^2 \frac{\partial \bar{u}}{\partial z} \right] \end{aligned} \quad (16)$$

and

$$\begin{aligned} \frac{\partial \tau_\eta}{\partial \xi} &= \frac{\partial}{\partial \xi} \left( \epsilon \frac{\partial v}{\partial \xi} \right) \\ &= \frac{U \epsilon \lambda}{d^2} \left[ 2 \left( 1 - \frac{1-z}{\epsilon} \frac{\partial \epsilon}{\partial z} \right) \bar{u} - (1-z) \left( 4 - \frac{1-z}{\epsilon} \frac{\partial \epsilon}{\partial z} \right) \frac{\partial \bar{u}}{\partial z} \right. \\ &\quad \left. + (1-z)^2 \frac{\partial^2 \bar{u}}{\partial z^2} \right] \end{aligned} \quad (17)$$

To eliminate the unknown eddy viscosity  $\epsilon$  and its derivative  $\partial \epsilon / \partial z$ , the  $\epsilon$  value is correlated with the streamwise shear stress such that

$$\tau_\xi = \epsilon \frac{\partial u}{\partial \xi} = \frac{U \epsilon}{d} \frac{\partial \bar{u}}{\partial z} \quad (18)$$

and

$$\begin{aligned} \frac{\partial \tau_\xi}{\partial \xi} &= \frac{\partial \epsilon}{\partial \xi} \frac{\partial u}{\partial \xi} + \epsilon \frac{\partial^2 u}{\partial \xi^2} \\ &= \frac{U \epsilon}{d^2} \left( \frac{1}{\epsilon} \frac{\partial \epsilon}{\partial \xi} \frac{\partial \bar{u}}{\partial z} + \frac{\partial^2 \bar{u}}{\partial z^2} \right) \end{aligned} \quad (19)$$

It is further assumed that the streamwise shear stress varies linearly across the boundary layer:

$$\tau_\xi = \tau_{\xi w} (1-z) = \frac{1}{2} \rho U^2 C_{f\ell} (1-z) \quad (20)$$

which yields

$$\frac{1}{\gamma M^2 P} \frac{\partial \tau_\xi}{\partial \xi} = -\frac{C_{f\ell}}{2d} \quad (21)$$

With the aid of relations (18) through (21), along with basic profiles (7) and (8), one obtains

$$\begin{aligned} \frac{1}{\gamma M^2 P} \frac{\partial \tau_\eta}{\partial \xi} &= \frac{C_{f\ell} \lambda (1-z)}{d} \left\{ \left( \frac{z}{h} - \frac{1-z}{2} \right) \times \right. \\ &\quad \left. \left[ 1 - \frac{(1-h)(1-z)}{z} \right] - 2(1-z) \right\} \end{aligned} \quad (22)$$

where  $z$  is set to  $d_1/d$  for actual calculations. The choice, although arbitrary, is considered to be the most appropriate in capturing the overall property of the boundary layer.

Equations (4) through (6) are coupled with Eqs. (1) through (3) and integrated simultaneously along a streamline. The fourth-order Runge-Kutta scheme is used in the numerical integration. To account for the crossflow derivatives, the integration is performed along at least two adjacent streamlines simultaneously. The differences in the resulting variables are then evaluated as the crossflow derivatives and immediately fed into the source terms of Eqs. (4) through (6); see Appendix. This whole procedure has been coded in BASIC language using an H-P 9836 desk-top computer. Calculated flow patterns are instantly displayed graphically to facilitate locating the streamline convergence.

### Results and Discussion

Numerical results are calculated for a prolate spheroid ( $a/b = 5.91$ ) at  $V_\infty = 45$  m/s (147.6 ft/s) and  $\alpha = 10$  and  $20$  deg. The flow is largely turbulent. In the calculation, the flow is tripped to turbulent at  $s/a = 0.1$ , where the initial conditions  $H = 1.35$ ,  $\Theta_{11} = 0.0005$ , and  $\lambda = 0$  are applied. Results of the streamwise shape factor  $H$  and the momentum thickness  $\Theta_{11}$  along streamlines of  $\eta = 1, 3, 10$ , and  $70$  for the case of  $\alpha = 10$  deg are shown in Figs. 3 and 4, respectively. The  $\Theta_{11}$  values rise significantly in all four streamlines as they proceed downstream. Nevertheless, the downstream flow exhibits reasonable stability as indicated by declining  $H$  values in that region.

Figures 5 and 6 show the calculated results of the streamwise skin friction coefficient  $C_{f\ell}$  and the direction of the wall shear stress  $\lambda$ , along the above streamlines. Comparison of the present  $C_{f\ell}$  values with those obtained by a finite difference scheme<sup>8</sup> and by experiment<sup>9</sup> is made. Agreement is within the range of the data scattering; see Fig. 5. The crossflow characteristics are represented by the value  $\lambda$  ( $\lambda = \tan \beta$ ). Generally,  $\lambda$  takes on a positive value in the upstream region and turns negative downstream; see Fig. 6. This indicates that the effect of viscosity makes the streamline steeper in the upstream region and flatter downstream compared with the external inviscid streamlines based on the potential flow theory; see Fig. 7. The trend is consistent with previous findings.<sup>10, 11</sup> The deflection of streamlines in the leeside that causes vortex-type separation is clearly portrayed.

Contrary to intuition, the deviation of viscous streamlines from the inviscid pattern does not stem from the shear stress derivative in Eq. (3), but rather is attributed to the deficiency of the velocity inside the boundary layer. In Fig. 8, the crossflow velocity profiles and the resulting shear stress derivatives are plotted at five locations along the streamline  $\eta = 3$ . At  $z = d_1/d$ , where the layer is set for the present computation, the numerical values for  $\partial \tau_w / \partial z / \gamma M^2 P$  from Eq. (22) are negative in the upstream region (Points A, B, and C in Fig. 8) then change to positive downstream (Points D and E). In fact, these friction values provide resistance to the change of the streamline direction from its external pattern.

The change in the sign of the wall shear angle from positive to negative implies that a zero crossflow skin friction line exists, since  $C_{f\eta} = \lambda C_{f\ell}$ . The calculated crossflow skin friction coefficients along these lines are presented in Fig. 9. Based on the framework of the present theory, this zero crossflow skin friction line (portrayed in Fig. 10) is apparently not a line of separation. This is in agreement with experimental observation.<sup>12</sup>

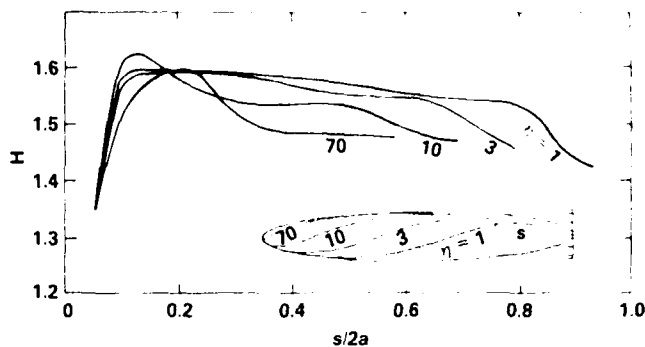


Fig. 3 - Streamwise boundary layer shape factor of flow over a prolate spheroid at  $\alpha = 10$  deg and  $V_\infty = 45$  m/s

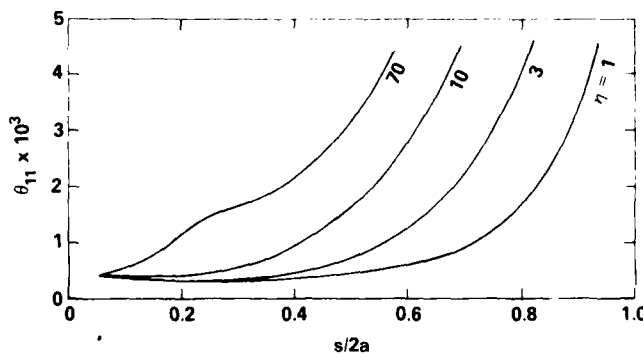


Fig. 4 - Streamwise momentum thickness of flow over a prolate spheroid at  $\alpha = 10$  deg and  $V_\infty = 45$  m/s

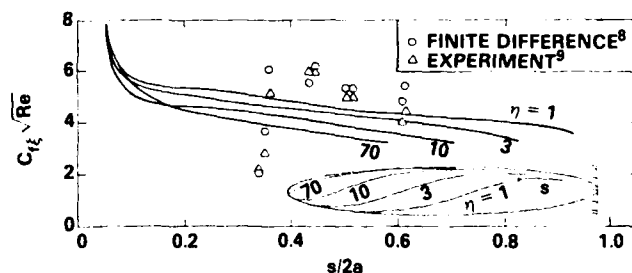


Fig. 5 - Streamwise skin friction coefficients of flow over a prolate spheroid at  $\alpha = 10$  deg and  $V_\infty = 45$  m/s

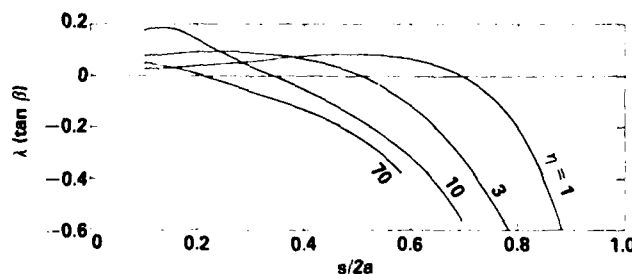


Fig. 6 - Direction of wall shear stress of flow over a prolate spheroid at  $\alpha = 10$  deg and  $V_\infty = 45$  m/s



The calculated overall flow pattern is shown in Fig. 10. The flow separation is detected near the rear stagnation region. The result is compared with that obtained by the limiting streamline pattern based on the measured wall shear stresses.<sup>13</sup> Agreement is very good. At the line of separation, which results from the formation of the envelope of viscous streamlines, the streamlines from the windside yield higher streamwise wall friction values than those from the leeward. This implies that the windside streamlines possess more energy and, therefore, will roll over those from the leeward. A similar conclusion was reached from the analysis based on the difference in velocity components at the edge of the boundary layer normal to the separation line.<sup>11</sup>

The result of the flow pattern at  $\alpha = 20$  deg is shown in Fig. 11. The line of separation emerges further in the upstream creating a larger separated region in the leeward of the flow. Although a direct comparison between calculated and experimental results cannot be made because of a lack of published data for this particular angle of attack, the present result does fall in between the measurements of the  $\alpha = 10$ - to 30-deg cases.<sup>12</sup>

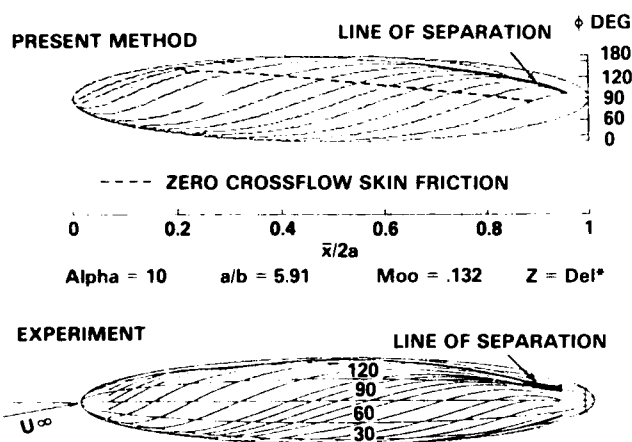


Fig. 10 - Flow separation pattern on a prolate spheroid at  $\alpha = 10$  deg and  $V_\infty = 45$  m/s

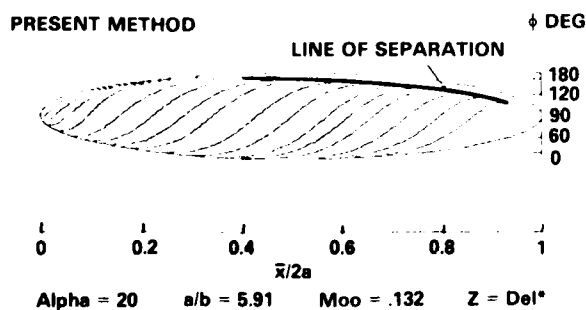


Fig. 11 - Flow separation pattern on a prolate spheroid at  $\alpha = 20$  deg and  $V_\infty = 45$  m/s

## Concluding Remarks

A three-dimensional integral boundary-layer approach is developed and coupled with the streamline method for theoretically determining the vortex-type flow separation. The deflection of leeward streamlines that causes the vortex-type separation is found to be attributed to the deficiency of velocity inside the boundary layer. The calculated theoretical results compare very well with the experimental data for the case of the prolate spheroid at  $\alpha = 10$  deg. For higher angle of attack, the approach yields qualitative agreement. The zero crossflow skin friction line exists, but it is not a line of separation.

## References

1. Tai, T.C., "Determination of Three-Dimensional Flow Separation by a Streamline Method," *AIAA Journal*, Vol. 19, No. 10, Oct 1981, pp. 1264-1271.
2. Tai, T.C., "Effect of Crossflow on the Vortex-Type Three-Dimensional Flow Separation," *Three-Dimensional Turbulent Boundary Layers*, edited by H.H. Fernholz and E. Krause, Springer-Verlag, 1982.
3. Cooke, J.C. and Hall, M.G., "Boundary Layers in Three Dimensions," *Progress in Aeronautical Sciences*, Volume 7, edited by A. Ferri, et al., Pergamon Press, 1962.
4. Mager, A., "Generalization of Boundary Layer Momentum Integral Equations to Three-Dimensional Flows Including Those of Rotating Systems," NACA Report 1067, 1962.
5. Smith, P.D., "An Integral Prediction Method for Three-Dimensional Compressible Turbulent Boundary Layers," R&M No. 3739, RAE, Dec 1972.
6. Green, J.E., "Application of Head's Entrainment Method to the Prediction of Turbulent Boundary Layers and Wakes in Compressible Flow," RAE Technical Report 72079, 1972.
7. DeJarnette, F.R. and Tai, T.C., "A Method for Calculating Laminar and Turbulent Heat Transfer Over Bodies at an Angle of Attack," NASA CR-101678, Mar 1969.
8. Ragab, S.A., "A Method for the Calculation of Three-Dimensional Boundary Layers with Circumferential Reversed Flow on Bodies," AIAA Paper No. 82-1023, Jun 1982.
9. Meier, H.U., and Kreplin, H.P., "Experimental Investigation of the Transition and Separation Phenomena on a Body of Revolution," *Z. Flugwiss. Weltraumforschung* 4, pp. 65-71, 1980.
10. Han, T. and Patel, V.C., "Flow Separation on a Spheroid at Incidence," *J. Fluid Mechanics*, Vol. 92, Part 4, 1979, pp. 643-657.
11. Tai, T.C., "Determination of Three-Dimensional Flow Separation Using Measured Pressure Distribution," AIAA Paper No. 83-0297, Jan 1983.
12. Meier, H.U., Kreplin, H.P., and Vollmers, H., "Velocity Distributions in 3-D Boundary Layers and Vortex Flows Developing on an Inclined Prolate Spheroid," *Proceedings of the 6th U.S.-West Germany Data Exchange Agreement Meeting on Viscous and Interacting Flow Field Effects*, Gottingen, Germany, Apr 1981, pp. 202-217.
13. Kreplin, H.P., Vollmers, H., and Meier, H.U., "Experimental Determination of Wall Shear Stress Vectors on an Inclined Prolate Spheroid," *Proceedings of the 5th U.S.-West Germany Data Exchange Agreement Meeting on Viscous and Interacting Flow Field Effects*, AFFDL-TR-80-3088, 1980, pp. 315-332.

# Appendix

Functions for  $G_1$ ,  $G_2$ , and  $G_3$

The detailed expressions for functions  $G_1$ ,  $G_2$ , and  $G_3$  in Eqs. (13) through (15) are listed below.

$$G_1 = A_1$$

$$G_2 = \frac{1}{\Theta_{11} Q_{21}} \left[ A_2 - A_1 E_{21} + \frac{R_{21}(A_1 E_0 - A_1 H - A_3)}{R_0 - 1} \right]$$

$$G_3 = \frac{A_3 - A_1(E_0 - H)}{\Theta_{11}(R_0 - 1)}$$

$$A_1 = B_1 - \frac{E_{12}}{h_2} \frac{\partial \Theta_{11}}{\partial \eta} - \Theta_{11} \left( \frac{Q_{12}}{h_2} \frac{\partial \lambda}{\partial \eta} + \frac{R_{12}}{h_2} \frac{\partial H}{\partial \eta} \right)$$

$$A_2 = B_2 - \frac{E_{22}}{h_2} \frac{\partial \Theta_{11}}{\partial \eta} - \Theta_{11} \left( \frac{Q_{22}}{h_2} \frac{\partial \lambda}{\partial \eta} + \frac{R_{22}}{h_2} \frac{\partial H}{\partial \eta} \right)$$

$$A_3 = B_3 + \frac{E_2}{h_2} \frac{\partial \Theta_{11}}{\partial \eta} + \Theta_{11} \left( \frac{Q_2}{h_2} \frac{\partial \lambda}{\partial \eta} + \frac{R_2}{h_2} \frac{\partial H}{\partial \eta} \right)$$

$$B_1 = \frac{C_{12}}{2} - \Theta_{11} \left[ \frac{(1 + E_1)}{U h_1} \frac{\partial U}{\partial \xi} + (2E_{21} - E_2) \left( K_1 + \frac{1}{U h_2} \frac{\partial U}{\partial \eta} \right) + (1 - E_{22}) K_2 \right]$$

$$B_2 = \frac{C_{12}}{2} - \Theta_{11} \left[ 2E_{21} \left( \frac{1}{U h_1} \frac{\partial U}{\partial \xi} + K_2 \right) + \frac{2E_{22}}{U h_2} \frac{\partial U}{\partial \eta} - (1 - E_{22} + H) K_1 \right]$$

$$B_3 = C_E - \Theta_{11} \left[ (E_0 - H) \left( \frac{1}{U h_1} \frac{\partial U}{\partial \xi} + K_2 \right) - E_2 \left( \frac{1}{U h_2} \frac{\partial U}{\partial \eta} + K_1 \right) \right]$$

$$\delta = E_0 \Theta_{11}$$

$$\delta_1 = E_1 \Theta_{11}$$

$$\delta_2 = E_2 \Theta_{11}$$

$$\Theta_{12} = E_{12} \Theta_{11}$$

$$\Theta_{21} = E_{21} \Theta_{11}$$

$$\Theta_{22} = E_{22} \Theta_{11}$$

$$E_0 = \frac{H(H+1)}{H-1}$$

$$E_1 = H$$

$$E_2 = -\lambda E_0 \left( \frac{2}{H+1} - \frac{4}{H+3} + \frac{2}{H+5} \right)$$

$$E_{12} = \lambda E_0 \left( \frac{1}{H} - \frac{4}{H+1} + \frac{1}{H+2} - \frac{4}{H+3} + \frac{2}{H+5} \right)$$

$$E_{21} = E_2 + E_{12}$$

$$E_{22} = -\lambda^2 E_0 \left( \frac{1}{H} - \frac{4}{H+1} + \frac{6}{H+2} - \frac{4}{H+3} + \frac{1}{H+4} \right)$$

$$Q_2 = \frac{\partial E_2}{\partial \lambda} = \frac{E_2}{\lambda}$$

$$Q_{12} = \frac{\partial E_{12}}{\partial \lambda} = \frac{E_{12}}{\lambda}$$

$$Q_{21} = \frac{\partial E_{21}}{\partial \lambda} = \frac{E_{21}}{\lambda}$$

$$Q_{22} = \frac{\partial E_{22}}{\partial \lambda} = \frac{E_{22}}{\lambda}$$

$$R_0 = \frac{\partial E_0}{\partial H} = \frac{H(H-2)+1}{(H-1)^2}$$

$$R_2 = \frac{\partial E_2}{\partial H} = \frac{E_2 R_0}{E_0} + \lambda E_0 \left[ \frac{2}{(H+1)^2} - \frac{4}{(H+3)^2} + \frac{2}{(H+5)^2} \right]$$

$$R_{12} = \frac{\partial E_{12}}{\partial H} = \frac{E_{12} R_0}{E_0} + \lambda E_0 \left[ \frac{1}{H^2} - \frac{4}{(H+1)^2} + \frac{1}{(H+2)^2} + \frac{4}{(H+3)^2} - \frac{2}{(H+5)^2} \right]$$

$$R_{21} = \frac{\partial E_{21}}{\partial H} = R_2 + R_{12}$$

$$R_{22} = \frac{\partial E_{22}}{\partial H} = \frac{E_{22} R_0}{E_0} + \lambda^2 E_0 \left[ \frac{1}{H^2} - \frac{4}{(H+1)^2} + \frac{6}{(H+2)^2} - \frac{4}{(H+3)^2} + \frac{1}{(H+4)^2} \right]$$

$$\frac{1}{h_2} \frac{\partial \Theta_{11}}{\partial \eta} \cong \left( \frac{\Delta \Theta_{11}}{h_2 \Delta \eta} \right)_\xi = \left[ \frac{(\Theta_{11})_{\eta+\Delta \eta} - (\Theta_{11})_\eta}{\Delta \eta} \right]_\xi$$

$$\frac{1}{h_2} \frac{\partial \lambda}{\partial \eta} \cong \left( \frac{\Delta \lambda}{h_2 \Delta \eta} \right)_\xi = \left( \frac{\lambda_{\eta+\Delta \eta} - \lambda_\eta}{\Delta \eta} \right)_\xi$$

$$\frac{1}{h_2} \frac{\partial H}{\partial \eta} \cong \left( \frac{\Delta H}{h_2 \Delta \eta} \right)_\xi = \left( \frac{H_{\eta+\Delta \eta} - H_\eta}{\Delta \eta} \right)_\xi$$

$$\frac{1}{h_1} \frac{\partial U}{\partial \xi} = \cos \theta \frac{\partial U}{\partial x} + \frac{\sin \theta}{f} \frac{\partial U}{\partial \phi}$$

$$\frac{1}{h_2} \frac{\partial U}{\partial \eta} = \frac{\cos \theta}{f} \frac{\partial U}{\partial \phi} - \sin \theta \frac{\partial U}{\partial x}$$

Errata: An Integral Prediction Method for  
Three-Dimensional Flow Separation

Tsze C. Tai

David Taylor Naval Ship Research and Development Center  
Bethesda, Maryland

[AIAA Paper No. 84-0014]

Equation (12) on page 3 of the paper should read:

$$K_2 = \frac{1}{h_1 h_2} \frac{\partial h_2}{\partial \xi}$$

$$= \frac{1}{\gamma M^2 P} \left( \frac{\partial P}{\partial x} \cos \theta + \frac{1}{f} \frac{\partial P}{\partial \phi} \sin \theta \right) + \frac{1}{U} \left[ \left( \frac{\partial u}{\partial x} + \frac{1}{f} \frac{\partial v}{\partial \phi} \right) + \frac{u}{f} \frac{df}{dx} \right]$$

Equations for  $B_1$  and  $Q_{22}$  in the Appendix of the paper should read:

$$B_1 = \frac{C_{f\xi}}{2} - \theta_{11} \left[ \frac{(2+E_1)}{U h_1} \frac{\partial U}{\partial \xi} + (2E_{21} - E_2) \left( K_1 + \frac{1}{U h_2} \frac{\partial U}{\partial \eta} \right) + (1-E_{22}) K_2 \right]$$

$$Q_{22} = \frac{\partial E_{22}}{\partial \lambda} = \frac{2E_{22}}{\lambda}$$

# INITIAL DISTRIBUTION

## Copies

2 OSD  
 1 Tech Library  
 1 R.F. Siewert (DDR&E)

4 CNR  
 1 211  
 1 430B  
 1 432  
 1 438

4 CNR  
 1 CNR, Boston  
 1 CNR, Chicago  
 1 CNR, London, England  
 1 CNR, Pasadena

1 NRL/Tech Library

1 USNA/Tech Library

1 NAVPGSCOL/Tech Library

1 NAVAIRDEVCEN/Tech Library

1 NAVWPNCEN/Tech Library

10 NAVAIRSYSCOM  
 1 AIR-03A  
 1 AIR-310  
 3 AIR-310D  
 1 AIR-530B  
 3 AIR-5301  
 1 AIR-7226/Tech Library

4 NAVSEASYSKOM  
 1 SEA 03R  
 1 SEA 55W3  
 1 SEA 63R  
 1 SEA 99612/Tech Library

1 NAPTC/Tech Library

1 PMTC/Tech Library

12 DTIC

## Copies

1 AFOSR/Aero Science

1 AFAL/Tech Library

1 AFFDL/Tech Library

4 NASA  
 1 HQ, Washington, D.C.  
 1 Ames Res Center  
 1 Langley Res Center  
 1 Lewis Res Center

1 NBS/Tech Library

1 NSF/Tech Library

## CENTER DISTRIBUTION

Copies	Code	Name
1	012.3	
1	15	
3	1606	Aerodynamics Collection
1	18	
10	5211.1	Reports Distribution
1	522.1	TIC (C) + 1m
1	522.2	TIC (A)



END

FILMED

8

24